2nd International Symposium on Magnetic Beaing
July 12-14, 1990, Tokyo, Japan

Vibration Control of Magnetically Suspended Flexible Rotor by the Use of Optimal Regulator

S.AKISHITA* T.MORIMURA* S.HAMAGUCHI**

*Department of Mechanical Engineering, Ritsumeikan University, Kita-ku, Kyoto 603, Japan
**NTN Corp. Iwata, Shizuoka 438, Japan

Abstract This paper proposes the application expansion of frequency shaped regulator to the vibration control of the flexible rotor supported by magnetic bearings. The dynamics of the flexible rotor is modeled as axi-symmetric slender shaft with FEM. The design method of the regulator containing the second order pre-filter of low-pass property is described applying the plant model of the flexible rotor and the radial magnetic bearings. The practical aspect of designing is examined for a flexible slender rotor of total length $520mm$. The regulator derived from the rotor model containing only two rigid-body modes proves effective for the vibration control of the rotor. The influence of the sampling rate of the controller and of the cut-off frequency of the filter are examined by the use of computer simulation.

1. INTRODUCTION

The use of magnetic suspension is increasing in its various forms with its proven high level of reliability, negligible maintenance and low energy consumption. The benefits come from the non-contact support which results in negligibly small friction and low vibration level of the supported body. Its use spreads from the high speed rail way vehicle to the rotational machinery. One of the most attractive advantages of the magnetic suspension is the applicability to the vibration control of the flexible suspended structure. The control system concerned with maintaining a floating gap is also applied to the vibration suppression. Modern machinery is apt to decrease of its weight and accordingly the stiffness. On the other hand the moving speed of the machinery consistently increases. These trends often result in the increase of the control band-width and the decrease of the natural frequency of the structure. Incidentally we are forced to solve the problem of the resonance between the structure and the control system.

In order to support a flexible rotor statbly by magnetic bearing, the suppressing of higher mode vibration else than two rigid-body mode is needed, although only four pairs of actuators are installed in magnetic suspension systems. This is a typical problem of spill-over avoidance in flexible structure. Direct feedback control[1] where colocated sensor signals are fed-back to actuators have been utilized. In a magnetic suspension system direct position feedback causes the positive spring and direct velocity feedback causes the damping effect. The design method of control systems concerns with assignment of the velocity feedback gains to the flexible vibration mode. The utilization of the pseudo inverse was proposed to determine the gain matrix to the excessive degrees of the mode[2,3].

A flexible rotor has other problems, the first of which is the variation of the natural frequencies with the rotational speed and the second of which is the estimation errors of those. One of reasonable and practical means to cope with the problems is the utilization of the controller which has low-pass property. Recently the design method of the frequency shaped optimal regulator was developed[4,5] and its application to flexible space structures was proposed[6]. The authors propose the expansion of its application to the flexible rotor suspended by magnetic bearing. The optimal regulator is designed to stabilize the two rigid-body modes which have the natural frequencies of null and its accurate mass property. For suppressing the flexible mode whirl which is not modeled at designing, the low-pass property of the the regulator is made use of.

In section 2 the modelling of the magnetic bearing and flexible rotor is described. The non-rotational model of the rotor is supposed. But we treat four-axis control type magnetic bearing as the model. Finite Element Method

(FEM) is adopted to represent the dynamics of the flexible rotor for its broad applicability. In section 3 the design method of the regulator is described, where multi-input multi-output control systems are supposed. In section 4 the practical aspect of the designing are designed; cut-off frequency in the filter and sampling rate in the digital controller. These are examined with computer simulation. The adequacy of the conroller designing is approved.

2. MODELLING

As mentioned above a 4-axis control type magnetic bearing is supposed in the paper. A schematical cross sectional view of the radical magnetic bearing is shown in Fig.1. One axis contorol magnet comprises a pair of coil-sand iron cores. The rotor center is displaced at x from its equilibrium position. The gaps in the left pole and the right pole are ξ_l and ξ_r respectivel. The atractive forces f_l,f_r generated in both sides are represented respectively by the currents i_l,i_r and the gaps as follows,

$$f_l = 0.5k_L(i_l/\xi_l)^2, \qquad f_r = 0.5k_L(i_r/\xi_r)^2 \tag{1}$$

$$k_l = \frac{\mu_0}{2}NA \tag{2}$$

where μ_0 is the magnetic permeability of free space , N the turn number in the coil and A the surface area in the pole. The common coefficient k_L is assumed between both electro-magnets . As the gaps at the equilibrium position are common such as $\xi_l = \xi_r = \xi_0$, the non-equilibrium gaps ξ_l and ξ_r are represented as follows,

$$\xi_l = \xi_0 + x, \qquad \xi_r = \xi_0 - x \tag{3}$$

Then the currents in both gaps are assumed as in the following equations.

$$i_l = i_0 + x, \qquad i_r = i_0 - x \tag{4}$$

where i_0 is the common bias current between both coils. The currents are meaningful only when they are positive. The resultant force F composed of f_l and f_r are deduced as follows,

$$F = -f_l + f_r = -\frac{k_L}{2}\left(\frac{i_0+i}{\xi_0+x}\right)^2 + \frac{k_L}{2}\left(\frac{i_0-i}{\xi_0-x}\right)^2 \tag{5}$$

The coil currents i_l,i_r are governed with the input voltages v_l,v_r across the coil by the following relations

$$\begin{cases} K_{cl}v_l = (i_l - i_0)R_{cl} + \frac{d}{dt}(L_l i_l) \\ K_{cr}v_r = (i_r - i_0)R_{cr} + \frac{d}{dt}(L_r i_r) \end{cases} \tag{6}$$

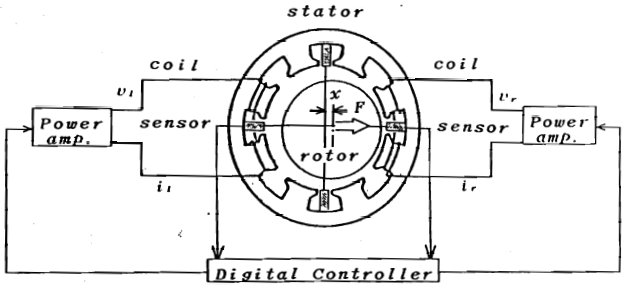

Fig.1 Cross sectional view of radial magnetic bearing

where

$$L_l = k_L/\xi_l, \qquad L_r = k_L/\xi_r \tag{7}$$

and, K_{cl} and K_{cr} are the voltage gains in the power amplifiers, R_{cl} and R_{cr} the resistances in both side coils. When the common voltage gains in the power amplifiers and the common resistances in the coils are assumed as,

$$K_c = K_{cl} = K_{cr} \tag{8}$$

$$R_c = R_{cl} = R_{cr} \tag{9}$$

Equation(6) is approximated as in the following, after the linearized expansion of ξ_l, ξ_r, i_l and i_l around their equilibrium conditions are introduced.

$$\begin{cases} K_c v_l = & R_c i & + \frac{k_L}{\xi_0}\dot{i} - \frac{k_L i_0}{\xi_0^2}\dot{x} \\ K_c v_r = & -R_c i & - \frac{k_L}{\xi_0}\dot{i} + \frac{k_L i_0}{\xi_0^2}\dot{x} \end{cases} \tag{10}$$

As v_l and v_r are correlated with each other, single variable v represents both variables as follows,

$$v = v_l = -v_r \tag{11}$$

when the coil current lag time, $T_0 = k_l/\xi_0 R_c$ is sufficiently short compared with the other dynamical characteristic time, we can simplify Eq.(10) as follows,

$$i = (K_c/R_c)v + (k_{Li}/R_c)\dot{x} \tag{12}$$

where k_{Li} is defined as follows,

$$k_{Li} = k_L(i_0/{\xi_0}^2) \tag{13}$$

The resultant force F can be approximated by using the similar linearization as follows,

$$F = -2k_{Li}i + 2k_{Lx}x \tag{14}$$

where k_{Lx} is defined as follows,

$$k_{Lx} = k_L({i_0}^2/{\xi_0}^3) \tag{15}$$

The bending motion of a flexible rotor is described by utilizing FEM. An axi-symmetric rotor is devided into n

components. The center point of i-th component is on $P(x_i, y_i)$ as shown in Fig.2. We assume that y_i is time-invariant. x_i means the radial displacement and it is represented as follows,

$$x_i = x_c + y_i\theta + w_i \tag{16}$$

where x_c is the displacement of the center of the gravity of the rotor, θ is the tilting angle of the rigid body mode, and w_i is defined as follows,

$$w = [x_c, \theta, w_1, w_2, \cdots, w_n]^T \tag{17}$$

The equation of the rotor motion is represented by the following,

$$M\ddot{w} + Kw = B'f \tag{18}$$

where M and K are the mass matrix and the stiffness matrix respectively. We should note that the dynamics of rotation is not considered in this paper. f is the force vector composed of the magnetic forces f_u, f_l at the upper bearing and the lower bearing respectively , as shown in the following equation.

$$f = [f_u, f_l]^T \tag{19}$$

Then, matrix B' is represented as follows,

$$B'^T = \begin{matrix} \\ 1 \\ 1 \end{matrix} \begin{matrix} \begin{matrix} (i_u) & & (i_l) & \end{matrix} \\ \begin{bmatrix} y_u & \cdots & 1 & \cdots & 0 & \cdots \\ y_l & \cdots & 0 & \cdots & 1 & \cdots \end{bmatrix} \end{matrix} \tag{20}$$

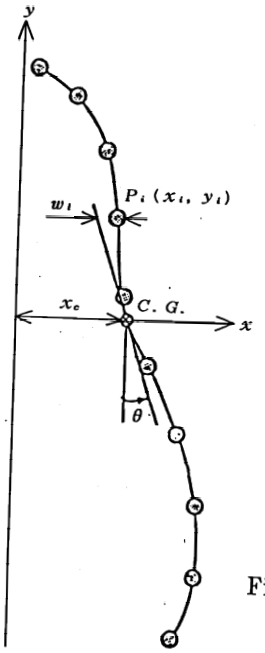

Fig.2 FEM model of flexible rotor

where y_u and y_l mean the y coordinate of the upper bearing and the lower bearing respectively, and they are on i_u component and on i_l component respectively. We transfer variable w to q with transfer matrix P as follows,

$$w = Pq \tag{21}$$

Then Eq.(18) is transferred to the decoupled equation as follows,

$$\ddot{q} + Lq = B_1 f \tag{22}$$

$$\begin{cases} L = diag.(0, 0, w_1^2, w_2^2, \cdots, w_n^2) \\ B_1 = P^T B' \end{cases} \tag{23}$$

Eq.(22) is applied to the computer simulation reserving the non-linearity in f_u and f_l represented by Eq.(5). But for designing the controller the linearly approximated equations, Eq.(12) and Eq.(14), are introduced. Then, Eq.(22) is transformed to the standard equation of the state retaining m flexible mode variables as follows,

$$\dot{x} = Ax + Bu \tag{24}$$

x is the state variable redefined as follows,

$$x = [x_c, \theta, q_1, \cdots, q_m, \dot{x_c}, \dot{\theta}, \dot{q_1}, \cdots, \dot{q_m}]^T \tag{25}$$

u is the input variable composed of the input voltages of the power amplifiers as follows,

$$u = [v_u, v_l]^T \tag{26}$$

Matrix A and B are rearranged as follows,

$$A = \begin{bmatrix} 0_m & \vdots & I_m \\ \cdots & \cdot & \cdots \\ A_1 & \vdots & A_2 \end{bmatrix} \tag{27}$$

$$A_1 = L_m + 2k_{Lx}\Phi B_{1m}^T$$
$$A_2 = (-2k_{Li}^2/R_c)\Phi B_{1m}$$

$$\Phi^T = \begin{bmatrix} P_{u1} & P_{u2}, & \cdots & , P_{um} \\ P_{l1} & P_{l2}, & \cdots & , P_{lm} \end{bmatrix} \tag{28}$$

$$B = -\frac{2k_{Li}K_c}{R_C}\begin{bmatrix} 0 \\ \cdots \\ B_{1m} \end{bmatrix} \tag{29}$$

where Φ is the mode shape matrix at magnetic bearings. The outputs of the system are the displacements of the center of i_u-th component and i_l-th component, as the colocation of the sensors and the actuators are assumed. The output equation is represented as follows,

$$y = Cx \tag{30}$$

$$C = \left[\Phi^T \ \vdots \ 0 \right] \tag{31}$$

3. CONTROL BY THE OPTIMAL REGULATOR

Imagine that the equilibrium of the flexible rotor suspension breaks down by some disturbance. Optimal regulator is utilized as the controller to restore the equilibrium and to maintain the stability of rotor suspension. When a plant model is represented by Eqs.(24) and (30), the following performance index J made up of an integral of quadrant forms is introduced.

$$J = \int_0^\infty [x^T C^T C x + u^T R^T R u] dt \tag{32}$$

On designing the conventional regulator R is time- invariant matrix independent upon angular frequency. The system input u is determined as $u = -kx$ so that the index J may be minimized. As R decreases, the higher gain and the frequency band-width pertains the controller. But if the model becomes obscure especially at high frequency range, the control system tends to unstable. For flexible rotor suspension systems some mode frequencies increase with the rotational speed. In order to preserve the robustness of the controller from the high-frequency uncertainty in the system model, we apply the optimal regulator reulting from frequency-shaped weight matrix. Equation (32) is transformed by using Perseval's theorem as follows,

$$J = \frac{1}{2\pi} \int_{-\infty}^{+\infty} \left[||Cx(i\omega)||^2 + ||Ru(i\omega)||^2 \right] d\omega \tag{33}$$

While C is assumed as time-invariant in the paper, R is treated as frequency-dependent as follows,

$$R^{-1}(i\omega) = \begin{bmatrix} r_{11}^{-1}(i\omega) & 0 \\ 0 & r_{22}^{-1}(i\omega) \end{bmatrix} \tag{34}$$

where $r_{11}^{-1}(i\omega)$ and $r_{22}^{-1}(i\omega)$ are defined as follows,

$$\begin{cases} r_{11}^{-1}(i\omega) = \omega_{01}^2/(s^2 + 2\zeta_{01}\omega_{01}s + \omega_{01}^2) \\ r_{22}^{-1}(i\omega) = \omega_{02}^2/(s^2 + 2\zeta_{02}\omega_{02}s + \omega_{02}^2) \end{cases} \tag{35}$$

$r_{11}^{-1}(i\omega)$ and $r_{22}^{-1}(i\omega)$ represent the low-pass property of 2nd order filter. ω_{01} and ω_{02} are the cut-off frequencies for u_l and u_r respectively. We introduce $v(i\omega)$ repersented as follows,

$$v(i\omega) = R(i\omega)u(i\omega) \tag{36}$$

From Eq.(34) it can be inferred that $R^{-1}(i\omega)$ represents the transfer matrix of low pass filter. Therefore, $v(i\omega)$ and $u(i\omega)$ are the input and output of low-pass pre-filter respectively, as shown in Fig.3(a). New state variable z is introduced to represent the internal description of the pre-filter as follows,

$$\dot{z} = A_F z + B_F v \tag{37}$$

$$u = C_F z \tag{38}$$

$$z = [z_1, z_2, \dot{z}_1, \dot{z}_2] \tag{39}$$

where A_F and B_F are represented as follows,

$$A_F = \begin{bmatrix} 0 & \vdots & I \\ \cdots & \cdot & \cdots \\ -D_1 & \vdots & -2G \end{bmatrix} \tag{40}$$

$$\begin{cases} C_1 = diag.(\zeta_{01}\omega_{01}, \zeta_{02}\omega_{02}) \\ D_1 = diag.(\omega_{01}^2, \omega_{02}^2) \end{cases}$$

$$B_F = \begin{bmatrix} 0 \\ \cdots \\ D_1 \end{bmatrix} \tag{41},$$

$$C_F^T = \begin{bmatrix} I \\ \cdots \\ 0 \end{bmatrix} \tag{42}$$

In order to construct the closed-loop of the extended system shown in Fig.3(a), we introduce the extended state variable $\bar{x}$ as follows,

$$\bar{x}^T = \left[x^T \ \vdots \ z^T \right] \tag{43}$$

The state equation of the extended system is represented as follows,

$$\dot{\bar{x}} = \bar{A}\bar{x} + \bar{B}v \tag{44}$$

where $\bar{A}$ and $\bar{B}$ are represented as follows,

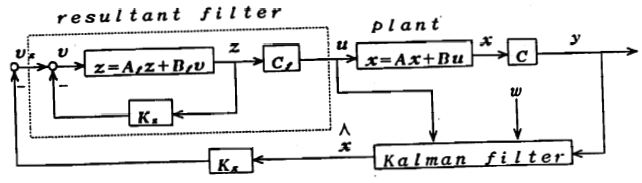

(a) extended system with prefilter

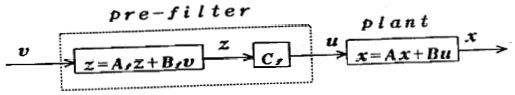

(b) closed-loop of frequency shaped regulator

Fig.3 Block diagram

$$\bar{A} = \begin{bmatrix} A & \vdots & BC_F \\ \cdots & \cdot & \cdots \\ 0 & \vdots & A_F \end{bmatrix} \quad (45), \qquad \bar{B} = \begin{bmatrix} 0 \\ \cdots \\ 0 \end{bmatrix} \quad (46)$$

Introducing the output matrix $\bar{C}$, which is time-invariant, as follows,

$$\bar{C} = \begin{bmatrix} C & \vdots & 0 \end{bmatrix} \quad (47)$$

the output equation of the extended system is represented as follows,

$$\bar{y} = \bar{C}\bar{x} \quad (48)$$

We can rearrange Eq.(33) for the extended system with new variables as follows

$$J = \frac{1}{2\pi}\int_0^\infty [||\bar{C}\bar{x}(i\omega)||^2 + ||v(i\omega)||^2]d\omega \quad (49)$$

after applying Parseval's theorem again, J is rewritten in time-domain as follows,

$$J = \int_0^\infty [\, \bar{x}^T\bar{C}^T\bar{C}\bar{x} + v^2 \,]dt \quad (50)$$

Since $\bar{x}$ and v are related with time-invariant weighting matrix($\bar{C}^T\bar{C}$ and I), the feedback gain can be determined with conventional design method for regulators as follows,

$$v = -\bar{B}^T P\bar{x} = -K_x x - K_z z \quad (51)$$

where P is determined from Ricatti's equation shown as follows,

$$\bar{A}^T P + P\bar{A} - P\bar{B}\bar{B}^T P + \bar{C}^T\bar{C} = 0 \quad (52)$$

As the controllability and observability of A, B and matrices are assumed for plant, the extended systems of $\bar{A}$, $\bar{B}$ and $\bar{C}$ can be stabilized.Then closed-loop of the frequency shaped regulator is composed as shown in block diagram of Fig.3(b). As the reduced oder model is applied for the plant, the output of the model contain the residual error w. Therefore Kalman filter is applied to estimate the state variable $\hat{x}$.

4. VIBRATION CONTROL ON FLEXIBLE ROTOR

We are discussing the practical aspect of the controller designing. The object is schematically shown in Fig.4. The slender rotor, which has a large disc in the midst, is suspended by an axial magnetic bearing and is supported radially by four radial magnetic bearings; the two at the upper end and other two at the lower position.

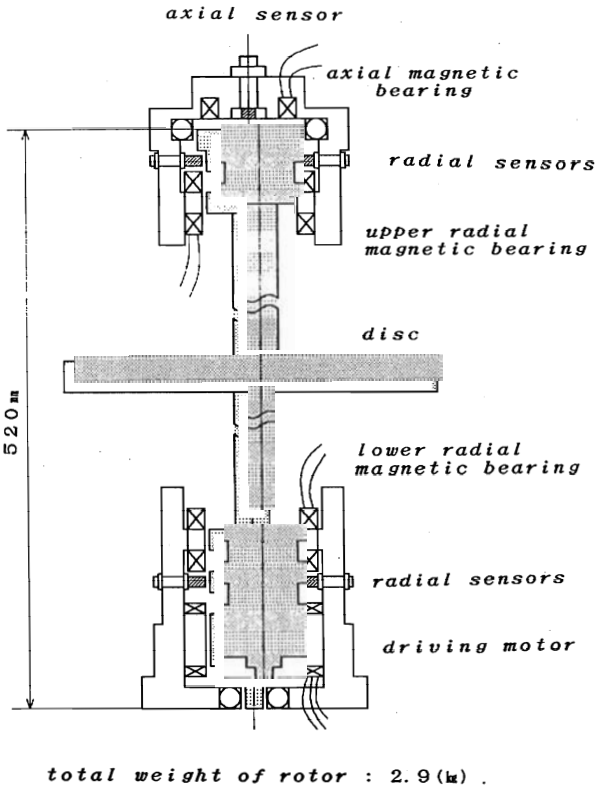

Fig.4 Schmatical cross-sectional view of 4-axis controlled magnetic bearing and suspended flexible rotor

The total length of rotor is about $520mm$ and its weight is about $3.0kg$ including a large disc. The rotor is modeled with FEM. The computational results of mode shape are shown in Fig.5. The first natural frequency of bending is $52Hz$. As the rotor is divided into 15 components, totally 15 eigen frequencies and eigen vectors are derived. But taking their significance and accuracy into consideration, first four modes are reserved at the computer simulation.

First designing of the frequency shaped regulator is executed by using the flexible rotor dynamics model which has two-rigid body modes and first two flexible modes. In case of the low-pass filter of $\omega_{01} = \omega_{02} = 251.3$ ($f_0 = 40Hz$) and $\zeta_{01} = \zeta_{02} = 0.5$ matrix $\bar{A}$, $\bar{B}$ and $\bar{C}$ are shown as in Appendix.The gap length $\xi_0 = 0.5\ mm$ and the bias current of the coil $i_0 = 0.5\ amp.$ are assumed for the magnetic bearing. Applying these matricies, gain matrix K of the regulator for extended systems are derived by using MATLAB toolbox as follows,

$$K_x = \begin{bmatrix} 63130 & -83420 & 2019 & 165.3 \\ 56810 & 47160 & -176.6 & 373.8 \end{bmatrix}$$

$$\begin{bmatrix} 566.4 & -728.7 & 12.46 & -0.1210 \\ 653.7 & 521.4 & -11.50 & 0.2828 \end{bmatrix}$$

$$K_z = \begin{bmatrix} 1.219 & -0.0203 & 0.0034 & -0.00005 \\ -0.0202 & 0.9000 & -0.00005 & 0.0027 \end{bmatrix} \quad (53)$$

The pole locations of the closed loop for the plant are derived from the eigen values of matrix $(A - BK_x)$ as shown in table.1.

$$\begin{cases} -1.269e-02 \pm 1.553e+03 \ i \\ -1.794e-02 \pm 3.065e+02 \ i \\ -2.386e+02 \\ -8.816e+01 \\ -1.605e+02 \\ -1.134e+02 \end{cases}$$

*table.*1

The adequacy of the regulator is proven with the computer simulation as shown in Fig.6 (a). The intial condition on the simulation is given, where the center of the rotor is displaced by $0.15mm$ (conically) and the input voltage is zero. On the simulation the sampling rate of the controller including the pre-filter can be given else than the simulation time division of Runge-Kutta solver. In this case the controller sampling rate $\Delta T = 0.5\ msec$ is assumed. Fig.6 (b) shows the variation of the input voltage of the upper electro-magnets. At the start of the simulation $x = 0.15\ mm$ and then the rotor is applied the attracting force to increase the displacement, while the input voltage of the electro-magnet does not rise. The rotor moves to the direction where the displacement enlarges till the input-voltage rises sufficiently and the restoring force rises at the pair of electro-magnets. After the controller works effectively the rotor is settled down at the equilibrium point within about 0.05 $msec$.

Further designing of the regulator is tried on the basis of simplest rotor dynamic model that contains only two rigid-body modes. The derived gain matrix K_x for regulator is shown as follows,

$$K_x = \begin{bmatrix} 63120 & -83400 & 566.6 & -728.9 \\ 56811 & 47160 & 653.6 & 521.5 \end{bmatrix} \quad (54)$$

where the same low-pass filter as the above is assumed. Comparing the gain matrix with that shown in Eq.(53) we find that the components for the rigid-body mode state variables are almost common between both gain matrices.

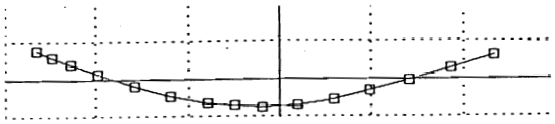

(a) 1st mode; 52 Hz

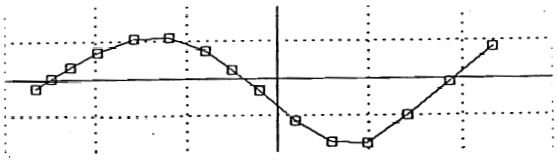

(b) 2st mode; 247 Hz

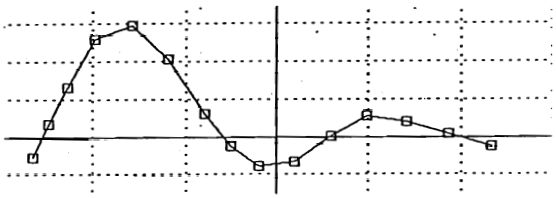

(c) 3st mode; 553 Hz

Fig.5 Mode shape of flexible rotor (FEM)

On the other hand, as the longer sampling rate in the controller is favourable, the computer simulation is excuted for the controller of the gain matrix of Eq.(54) assuming the sampling rate $\Delta T = 2\ msec$. We can find from Fig.7 that the stabilized rotor motion is assured though the settling time elongates compared with the case shown in Fig.6 (a). The influence of the filter cut-off frequency is interesting. The simulation result is shown in Fig.8 for cut-off frequency $f_0 = 25\ Hz$ and the same sampling rate. The rotor motion is stabilized not only for the initial displacement but also for the disturbace of 80 Hz imposed on $t = 0.20\ sec$ during one fouth of its period. We should add that for the longer sampling rate $\Delta T = 3\ msec$, the controller is effective. As the cut-off frequency f_0 decreases, the lag time at the input voltage rise increases and finally the rotor fails in restoring the equilibrium condition. A typical sample for the case of $f_0 = 10\ Hz$ is shown in Fig.9 (a) (b).

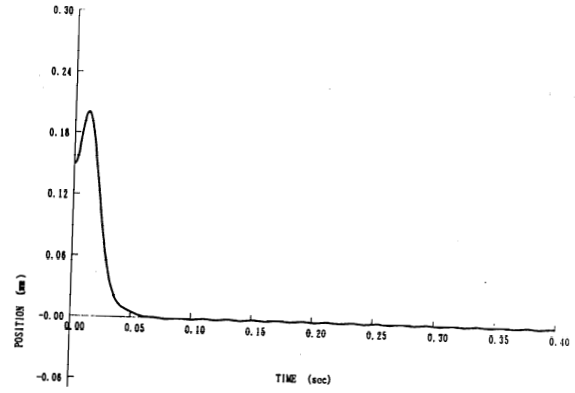

(a)rotor displacement

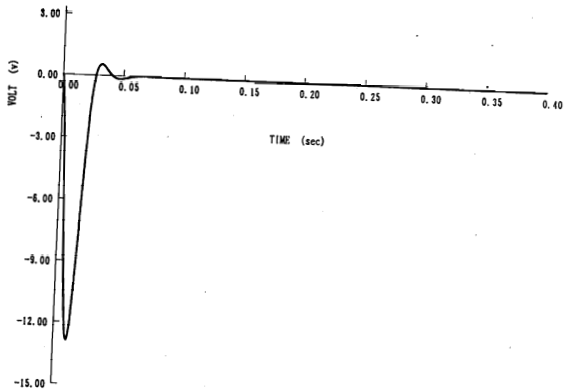

(b)input voltage

Fig.6 Vibration control by the regulator
$f_0 = 40\ Hz, \quad \Delta T = 0.5\ msec$

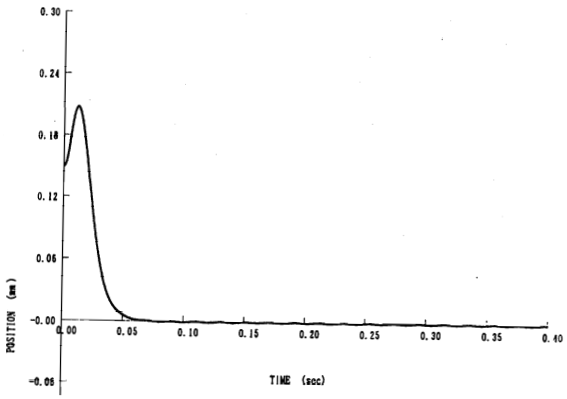

Fig.7 Vibration control by the regulator designed on the simplest model; rotor displacement
$f_0 = 40\ Hz, \quad \Delta T = 2.0\ msec$

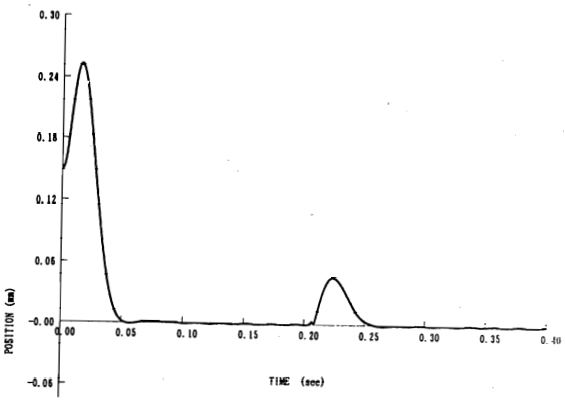

Fig.8 Vibration control by the regulator; rotor displacement
$f_0 = 25\ Hz, \Delta T = 2.0\ msec$

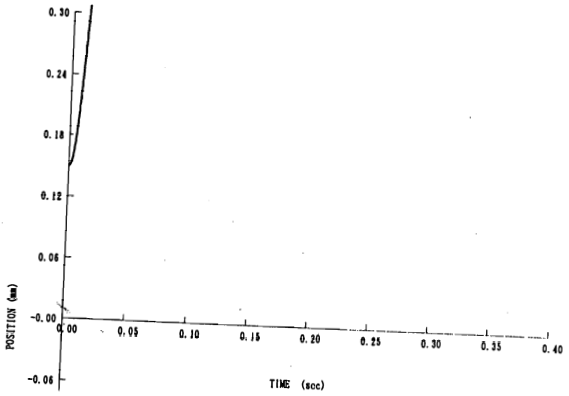

(a) rotor displacement

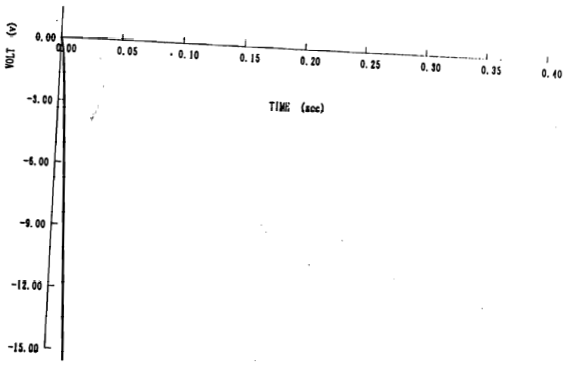

(b) input voltage

Fig.9 Vibration control by the regulator;
$f_0 = 10\ Hz, \Delta T = 2.0\ msec$

5. CONCLUSION

The effectiveness of the regulator containing the pre-filter of low pass property was verified for suppressing the vibration of the flexible rotor supported by magnetic bearings by using computer simulation. The regulator was derived from the rotor model containing only two rigid-body modes. The influences of the controller sampling rate and of the cut-off frequency of the pre-filter were examined. We can conclude that the frequency shaped regulator is applicable for controlling the flexible rotor support by magnetic bearigs, even if the accurate dynamic models of the flexible modes are not accessible. The regulator applicability will be verified on the experiment of the systems at near future.

REFERENCE

1. M.J.Balas, "Feed-back Control of Flexible System ", IEEE Transactions on Automatic Control, Vol.AC-23, No.4, pp.673, 1978
2. J.R.Salm, "Active Electromagnetic Suspension of an Elastic Rotor; Modelling, Control and Experimental Results ", Transactions of the ASME, Journal of Vibration, Acoustics, Stress and Reliability in Design", Vol.110, pp.493, 1988.
3. S.Akishita and K.Hayashi, "Vibration Control on Magnetically Suspended Flexible Beam ", the 1990 ASME Computers in Engineering Meeting in Boston, (to appear).
4. N.K.Gupta, "Frequency-Shaped Cost Functionals: Extension of Linear-Quadratic-Gaussian Design Methods ", Journal of Guidance and Control, Vol.3, No.6, pp.529, 1980.
5. B.D.O.Anderson and D.L.Mingori, "Use of Frequency Dependence in Linear Quadratic Control Problems to Frequency-Shape Robustness ", Journal of Guidance and Control, Vol.8, No.3, pp.447, 1985.
6. T.Kida, M.Ikeda and I.Yamaguchi, "Optimal Regulator with Low-Pass Property and Its Application to LSS Control ", Transactions of the Society of Instrument and Control Engineers, Vol.25, No.4, pp.448, 1989, (in Japanese).

APPENDIX

$$\bar{A} = \begin{bmatrix}
0.0 & 0.0 & 0.0 & 0.0 & 1.0 & 0.0 & 0.0 & 0.0 & 0.0 & 0.0 & 0.0 & 0.0 \\
0.0 & 0.0 & 0.0 & 0.0 & 0.0 & 1.0 & 0.0 & 0.0 & 0.0 & 0.0 & 0.0 & 0.0 \\
0.0 & 0.0 & 0.0 & 0.0 & 0.0 & 0.0 & 1.0 & 0.0 & 0.0 & 0.0 & 0.0 & 0.0 \\
0.0 & 0.0 & 0.0 & 0.0 & 0.0 & 0.0 & 0.0 & 1.0 & 0.0 & 0.0 & 0.0 & 0.0 \\
8974 & -2214 & 818.5 & 465.0 & -4.395 & 1.084 & -0.401 & -0.228 & 0.227 & 0.227 & 0.0 & 0.0 \\
-2203 & 10650 & -1267 & 786.6 & 1.079 & -5.217 & 0.621 & -0.385 & -0.297 & 0.186 & 0.0 & 0.0 \\
409.1 & -634.1 & -93910 & -26.31 & -0.200 & 0.311 & -0.046 & 0.013 & 0.023 & -0.002 & 0.0 & 0.0 \\
232.4 & 393.1 & -26.31 & -2412300 & -0.114 & -0.192 & 0.013 & -0.026 & -0.0049 & 0.017 & 0.0 & 0.0 \\
0.0 & 0.0 & 0.0 & 0.0 & 0.0 & 0.0 & 0.0 & 0.0 & 0.0 & 0.0 & 1.0 & 0.0 \\
0.0 & 0.0 & 0.0 & 0.0 & 0.0 & 0.0 & 0.0 & 0.0 & 0.0 & 0.0 & 0.0 & 1.0 \\
0.0 & 0.0 & 0.0 & 0.0 & 0.0 & 0.0 & 0.0 & 0.0 & -63170 & 0.0 & -251.3 & 0.0 \\
0.0 & 0.0 & 0.0 & 0.0 & 0.0 & 0.0 & 0.0 & 0.0 & 0.0 & -63170 & 0.0 & -251.3
\end{bmatrix}$$

$$\bar{B} = \begin{bmatrix}
0.0 & 0.0 \\
0.0 & 0.0 \\
0.0 & 0.0 \\
0.0 & 0.0 \\
0.0 & 0.0 \\
0.0 & 0.0 \\
0.0 & 0.0 \\
0.0 & 0.0 \\
0.0 & 0.0 \\
0.0 & 0.0 \\
63165 & 0.0 \\
0.0 & 63165
\end{bmatrix}, \quad \bar{C}^T = \begin{bmatrix}
0.5803 & 0.5803 \\
-0.7592 & 0.4729 \\
0.1179 & -0.0121 \\
-0.0248 & 0.0850 \\
0.0 & 0.0 \\
0.0 & 0.0 \\
0.0 & 0.0 \\
0.0 & 0.0 \\
0.0 & 0.0 \\
0.0 & 0.0 \\
0.0 & 0.0 \\
0.0 & 0.0
\end{bmatrix}$$